Biosensors and Bioelectronics 155 (2020) 112100

Contents lists available at ScienceDirect

Biosensors and Bioelectronics

journal homepage: http://www.elsevier.com/locate/bios

Surpassing the detection limit and accuracy of the electrochemical DNA sensor through the application of CRISPR Cas systems

Wei Xu [a], Tian Jin [d], Yifan Dai [b,c,*], Chung Chiun Liu [b,c]

[a] Department of Biomedical Engineering, Case Western Reserve University, Cleveland, OH, 44106, USA
[b] Department of Chemical and Biomolecular Engineering, Case Western Reserve University, Cleveland, OH, 44106, USA
[c] Electronics Design Center, Case Western Reserve University, Cleveland, OH, 44106, USA
[d] College of Biological Sciences, University of California, Davis, CA, 95616, USA

ARTICLE INFO

Keywords:
CRISPR biosensor
Electrochemical biosensor
ssDNA virus
DNA sensor
Point-of-care
Cas12a/Cas9

ABSTRACT

Robust developments of personalized medicine for next-generation healthcare highlight the need for sensitive and accurate point-of-care platforms for quantification of disease biomarkers. Broad presentations of clustered regularly interspaced short palindromic repeats (CRISPR) as an accurate gene editing tool also indicate that the high-specificity and programmability of CRISPR system can be utilized for the development of biosensing systems. Herein, we present a CRISPR Cas system enhanced electrochemical DNA (E-DNA) sensor with unprecedented sensitivity and accuracy. The principle of the E-DNA sensor is the target induced conformational change of the surface signaling probe (containing an electrochemical tag), leading to the variation of the electron transfer rate of the electrochemical tag. With the introduction of CRISPR cleavage activity into the E-DNA sensor, a more apparent signal change between with and without the presence of the target can be achieved. We compared the performance of Cas9 and Cas12a enhanced E-DNA sensor and optimized the chemical environment of CRISPR, achieving a femto-molar detection limit without enzymatic amplification. Moreover, we correlated the CRISPR cleavage signal with the original E-DNA signal as a strategy to indicate potential mismatches in the target sequence. Comparing with classic DNA electrochemistry based mutation detection strategy, CRISPR enhanced E-DNA sensor can determine the presence of a single mutation at an unknown concentration condition. Overall, we believe that the CRISPR enhanced E-DNA sensing strategy will be of especially high utility for point-of-care systems owing to the programmability, modularity, high-sensitivity and high-accuracy.

1. Introduction

The increasing understanding of critical physiological pathways for disease progression significantly promotes the development of personalized medicine, which is the key for next-generation healthcare industry, further leading to a society of better health (Ng et al., 2009). A simple, rapid detection system that can identify the morbigenous genes will be of especially high-utility for the design of personalized medicine (Yang and Gao, 2019). Among the advancements of various types of biosensing platforms, the electrochemical biosensing systems have been robustly developed in the last decade (Blair and Corrigan, 2019; Dai et al., 2019a; Dai and Liu, 2019), owing to the cost-effectiveness of the transduction system, the time-efficiency and the simplicity of sample processing, providing a potential deployable point-of-care system (Furst et al., 2013, 2014; Kelley et al., 2014; Kim et al., 2019; Labib et al., 2016; Li et al., 2019; Lubin and Plaxco, 2010; Pan et al., 2019; Povedano et al., 2018; Wei et al., 2019). One of the most successful contributions for the electrochemical biosensing system is the development of the E-DNA biosensor (Fan et al., 2003), which utilizes the conformational change of the surface probe upon the recognition of the target, inducing the change of electrochemical signal through the variation of contact-mediated electron transfer distance (Arroyo-Currás et al., 2018; Dauphin-Ducharme et al., 2019; Fan et al., 2005; Ferguson et al., 2013; Hsieh et al., 2012; Kang et al., 2018; Li et al., 2010, 2016, 2017; Song et al., 2008; Vallée-Bélisle et al., 2012; Zuo et al., 2007). The change of electrical signal before and after the introduction of the target (signal gain) depends on the quantity of hairpin surface probes opened by the target nucleic acid. Various studies have demonstrated the enhancement of signal gain through tuning different factors, such as voltammetric parameters (Dauphin-Ducharme and Plaxco, 2016; White and Plaxco,

* Corresponding author. Department of Chemical and Biomolecular Engineering, Case Western Reserve University, Cleveland, OH, 44106, USA.
E-mail address: yxd176@case.edu (Y. Dai).

https://doi.org/10.1016/j.bios.2020.112100
Received 14 January 2020; Received in revised form 12 February 2020; Accepted 13 February 2020
Available online 18 February 2020

2010), surface passivation condition and probe density (White et al., 2008), stem composition of the hairpin probe (Kang et al., 2012), in order to achieve an ideal conformational change for a satisfied sensing performance. These detail experimental tunings might limit the general programmability and applicability of the system and therefore highlight the need for a strategy that uncouples the challenge for an absolute signal gain and thus, surpassing the detection limit of E-DNA sensor.

From the idealized chemistry perspective, the ultimate signal gain would be the elimination of the electrochemical signal in the presence of the target, indicating that the removal of the electrochemical tag upon the target recognition is desirable. Recent discoveries of clustered regularly interspaced short palindromic repeats (CRISPR) Cas systems actually provide the opportunity to produce an absolute signal gain through the programmable and specific RNA guided cleavage activity (Chen et al., 2018; English et al., 2019; Gootenberg et al., 2017, 2018; Pardee et al., 2016). The CRISPR Cas system, as a powerful gene-editing tool (Chen and Doudna, 2017; Zetsche et al., 2015), performs the high-specificity recognition activity through the Cas enzyme-gRNA duplex and the following cleavage activity on the target DNA through the Cas enzyme (Bruch et al., 2019; Dai et al., 2019b), therefore providing the occupancy on the genome to allow the cell to operate its own repair mechanism (Mali et al., 2013; Sundaresan et al., 2017), achieving genome editing. We hypothesized that through the utilization of the target recognition induced cleavage activity of CRISPR for E-DNA sensor, the nucleic acid target and its complement (opened hairpin containing the electrochemical tag) can be cleaved by Cas enzyme, therefore releasing the electrochemical tag from the sensor surface. This process leads to an absolute loss of the signal, therefore surpassing the detection limit.

Moreover, a biosensing strategy that can discriminate point mutation would be of great meaning for genetic disorder analysis. However, current electrochemical mutation detection strategies mostly depend on the variation of DNA medicated charge transport process, which can only indicate mutations through signal comparison between wild-type and mutated sequences at same concentration of the targets (Boon et al., 2000; Kelley et al., 1999). Because without knowing the concentration of the target, the decreased current output of E-DNA sensor can be explained as either increased well-matched target concentration or the presence of the mutation, therefore not practical for clinical application for mutation evaluation. To resolve this issue, we further hypothesized that the incorporation of target complementarity dependent CRISPR cleavage activity into the E-DNA sensor allows a second-time recognition activity with a corresponding complementarity dependent cleavage signal, which can be combined with E-DNA sensor conformational change induced signal to indicate the presence of mutation without knowing the target concentration, therefore surpassing the detection accuracy and providing a unique strategy for mutation analysis.

In this work, we introduce a new concept based on the combination of electrochemistry based DNA sensor and CRISPR, delivering an integrated sensor and actuator system as a powerful biosensing platform. The designed CRISPR enhanced E-DNA sensor was demonstrated for the detection of a ssDNA virus, Parvovirus B19 (PB-19), which is known to cause erythema infectiosum in children and pregnant women (Young and Brown, 2004). We believe that owing to the generality and the continuous discoveries of CRISPR and its analogs, this CRISPR -mediated E-DNA sensing strategy can be widely adopted by future researches to boost the detection limit and accuracy for all the types of point-of-care systems.

2. Experimental

2.1. Fabrication of E-DNA sensor

An array of 20 sensors was cleaned through an established cleaning protocol (Dai et al., 2018). 5' modified C6 S-S linked synthetic hairpin probe was treated with 10 μM of tris(2-carboxyethyl)phosphine (TCEP) to reduce the S-S bond for 30 min in the dark at room temperature. After treatment, the thiol linked hairpin probe was diluted to 0.8 μM using 10 mM Tris buffer containing 100 mM NaCl, 10 mM $MgCl_2$ and 10 mM EDTA. The diluted hairpin probe was directly incubated onto the sensor array for 3 h at room temperature in the dark. Upon completion of the hairpin monolayer formation, the electrodes were passivated with 2 mM of 11-mercapto-1-undecanol (11-MCD) overnight at 4 °C. The electrodes were immersed and rinsed by 10 mM Tris buffer to remove any non-absorbed residual molecules before applying to target incubation. 20 μL of different concentrations of ssDNA targets were incubated onto the sensor array for 20 min before CRISPR treatment.

2.2. CRISPR treatment

2.2.1. Assembly of CRISPR Cas9-gRNA duplex

100 nM of Recombinant S. pyogenes Cas9 and sgRNA was assembled in 50 mM NaCl, 10 mM Tris-HCl, 10 mM $MgCl_2$, 100 μg/ml BSA (pH 7.9) at ambient temperature for 10 min. After formation of the CRISPR Cas9-gRNA duplex, 20 μL of the 100 nM of Cas9-gRNA duplex was applied directly onto the E-DNA sensor (after target capture) for incubation of 20 min at 37 °C to perform the cleavage activity. After CRISPR Cas9 system treatment, the sensor array was cleaned by immersing in 10 mM Tris buffer and dried by nitrogen gas. 80 U/mL of proteinase k was applied to the sensor array to digest the Cas enzymes for 10 min at 37 °C, preventing non-specific absorptions on the electrodes. After proteinase K treatment, the sensor array was cleaned by immersing in 10 mM Tris buffer and dried by nitrogen gas and ready for electrochemical test.

2.2.2. Assembly of CRISPR Cas12a-crRNA duplex

100 nM of LbCas12a and crRNA was assembled in 50 mM NaCl, 10 mM Tris-HCl, 10 mM $MgCl_2$, 100 μg/ml BSA (pH 7.9) at ambient temperature for 10 min. 20 μL of the 100 nM Cas12a-crRNA duplex was incubated onto the E-DNA sensor (after target capture) for incubation of 20 min at 37 °C to perform the cleavage activity. After CRISPR Cas12a system treatment, the sensor array was cleaned by immersing in 10 mM Tris buffer and dried by nitrogen gas. 80 U/mL of proteinase k was applied to the sensor array to digest the Cas enzymes for 10 min at 37 °C, preventing non-specific absorptions on the electrodes. After proteinase K treatment, the sensor array was cleaned by immersing in 10 mM Tris buffer and dried by nitrogen gas and ready for electrochemical test. For testing on human serum sample, pooled healthy human serum was used to spike different concentrations of the nucleic acid target into the sample and evaluated based on the same protocol as described above. All the nucleic acids used in this study are shown in Table S2.

2.3. Square wave voltammetry (SWV) investigation

For SWV test, a 10 mM Tris buffer containing 1 M NaCl was applied as the electrolyte. Square wave voltammetry (SWV) was applied before and after certain treatments to obtain the change of current based on a potential range of −0.1 V to −0.3 V (vs. Ag/AgCl) with a frequency of 5 Hz and an amplitude of 25 mV.

3. Results and discussion

A micro-fabricated, three-electrode, single-use sensor array was applied for the development of the biosensing system (Fig. S1). The principle of the sensing chemistry is illustrated in Fig. 1. A hairpin probe is attached to the electrode surface through 5′ end modified thiol moiety physically absorbed onto gold surface with a 3′end modified methylene blue electrochemical signaling tag (Fig. 1A). The presence of the target ssDNA opens the hairpin, delivering a longer electron transfer distance of the electrochemical tag (Fig. 1B). At this stage, a differentiable electrochemical signal is already acquirable between before and after the introduction of the target nucleic acid to the sensor. For the purpose to

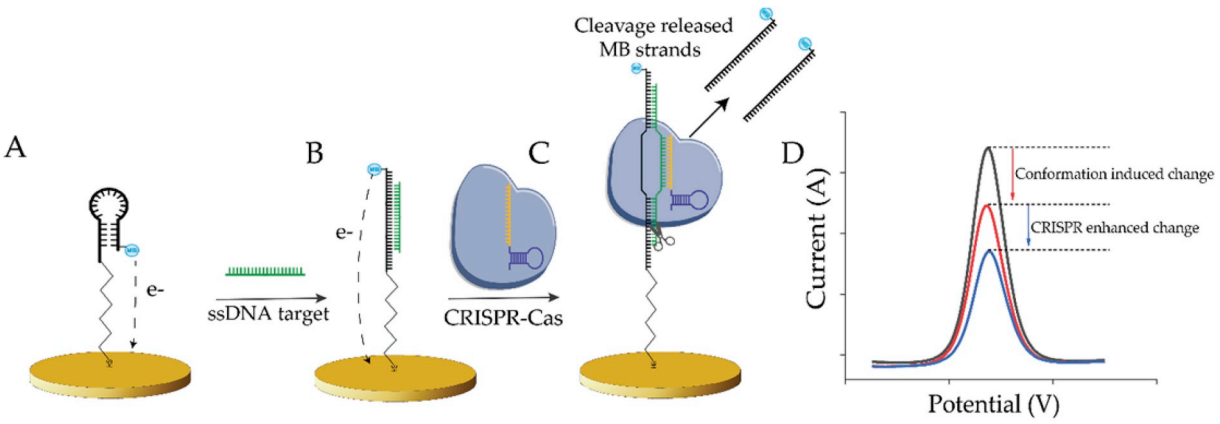

Fig. 1. Principle of CRISPR enhanced E-DNA sensor. (A) Construction of hairpin signaling strand on the gold electrode. (B) Addition of target opens the hairpin probe, increasing the electron tunneling distance. (C) Addition of CRISPR-Cas system performs a complementarity dependent cleavage activity, further releasing the electrochemical signaling probe from the electrode surface.(D) Representation of electrochemical current outputs based on the conformation change induced signal change and the CRISPR cleavage induced signal change.

enhance the signal gain, RNA guided CRISPR system can be programmed to recognize the formed dsDNA. Upon the second-time confirmation of the sequence information by CRISPR, cleavage activity is activated to remove the electrochemical tag conjugated DNA probe off the electrode (Fig. 1C), further enhancing the signal gain (Fig. 1D). Moreover, the CRISPR cleavage activity depends on the sequence complementarity with the guide RNA, so probing the CRISPR cleavage signal can lead to the indication of mutations in the target sequence, surpassing the detection accuracy of the conventional electrochemical DNA sensor.

3.1. Optimization of the E-DNA sensor

Before applying the CRISPR system onto the E-DNA sensor, we first optimized the detection performance of the E-DNA sensor through manipulating the surface density of the hairpin probe, the passivation agent, and the parameter of square wave voltammetry (SWV). SWV was applied to evaluate the methylene blue signal change before and after the incubation of the target ssDNA due to the change in the rate of the contact-mediated electron transfer process (Fig. S2) (Dauphin-Ducharme et al., 2019). The hairpin surface density was manipulated through the change of the concentration of the incubation solution; the greatest degree of change of signal was identified at the incubation concentration of 0.8 μM (Fig. S3). We further examined the effect of passivation agents with different lengths on the enhancement of the signal gain. 11-mercapto-1-undecanol (11-MCD) demonstrated the most stable and the greatest degree of current change before and after the introduction of the target (Fig. S4A). This might cause by the following reason. The hairpin immobilization linker is a 6-carbon chain. A longer carbon chain from 11-MCD can sterically limit the electrostatic repulsion between the phosphate backbones of the hairpin molecules (Fig. S4B). Therefore, the long passivation agent sustains the unfolding process of the hairpin probe more favorably than the short passivation agents, providing a stable, extended duplex structure with the introduction of the target and further delivering a greater change of electron transfer distance (Fig. S4B). Thus, 11-MCD was selected as the passivation agent for the development of the E-DNA sensor. Furthermore, the frequency of SWV was demonstrated playing a key role in signal on/off scenarios due to the internal electron transfer rate of the electrochemical probe (Dauphin-Ducharme and Plaxco, 2016). The least variation of signal was observed at a frequency of 5 Hz with an amplitude of 0.025 V (Fig. S5), which was then selected as the optimized frequency for the electrochemical test. The optimized conditions for E-DNA sensor was then applied to CRISPR treatment for performance enhancement.

3.2. Evaluation of CRISPR Cas9 for the E-DNA sensor performance enhancement

We first evaluated our designed detection strategy through the classic CRISPR-Cas9 system (from *Streptococcus pyogenes*), which is a type II CRISPR system (Hsu et al., 2014). Cas9 is a dual-RNA guided DNA endonuclease (Jinek et al., 2012), consisting of three elements (Fig. 2A): a crRNA: guiding for DNA cleavage, a tracrRNA: non-coding RNA to process the crRNA into the discrete ternary Cas9 complex, a Cas9 enzyme: cleaving target through the HNH domain and RuvC like domain (Jinek et al., 2012). The sensing/recognition part of CRISPR-Cas9 system is achieved by two parts: first, the confirmation of a short motif sequence referenced as the protospacer adjacent motif (PAM), 5′ NGG; second, the programmable crRNA guided target sequence recognition through the complementary base pairs. The integration of crRNA and tracrRNA is named as gRNA duplex. The actuator part is processed by gRNA guided Cas9 enzyme to perform the dsDNA cleavage at the position of 3 base-pair upstream of 5' PAM region and this cleavage activity is probed through electrochemistry (Fig. 2B). Based on the optimized E-DNA sensor condition, SWV was applied to evaluate the change of current outputs before and after the treatment by CRISPR-Cas9 (Fig. 2C). In response to 500 pM ssDNA target, CRISPR enhanced E-DNA sensor ($\Delta I_b\% = 59.1\%$) demonstrated an increasing change of current over the conventional E-DNA sensor ($\Delta I_a\% = 49.7\%$), indicating the effectiveness of the cleavage activity of Cas9 for on-chip *in vitro* cleavage. We further compared the sensing performance at low concentration range using E-DNA sensor and Cas9 enhanced E-DNA sensor (Fig. 2D). CRISPR-Cas9 enhanced E-DNA sensor demonstrated a higher detection resolution over the E-DNA sensor at pico-molar concentration level. Moreover, CRISPR-Cas9 enhanced E-DNA sensor surpassed the detection limit of the E-DNA sensor by at least two order of magnitudes. A differentiable signal can even be acquired between 1000 fM and 100 fM. The dynamic detection range of CRISPR enhanced E-DNA sensor was then examined (Fig. 2E). A IC50 value of 66.1 pM was obtained with an average standard error (SE) of 3.2%, indicating an excellent stability and sensitivity of this sensing platform.

3.3. Comparison of the performance of CRISPR Cas12a and Cas9 enhanced E-DNA Sensor

We further explored a different class of CRISPR, type V CRISPR-Cas system, Cas12a to evaluate its effect on enhancing the performance of the E-DNA sensor. Distinct from CRISPR-Cas9, Cas12a performs dsDNA cleavage with a single RuvC catalytic domain guided by its own crRNA, providing a simpler system than Cas9(Chen et al., 2018). The PAM

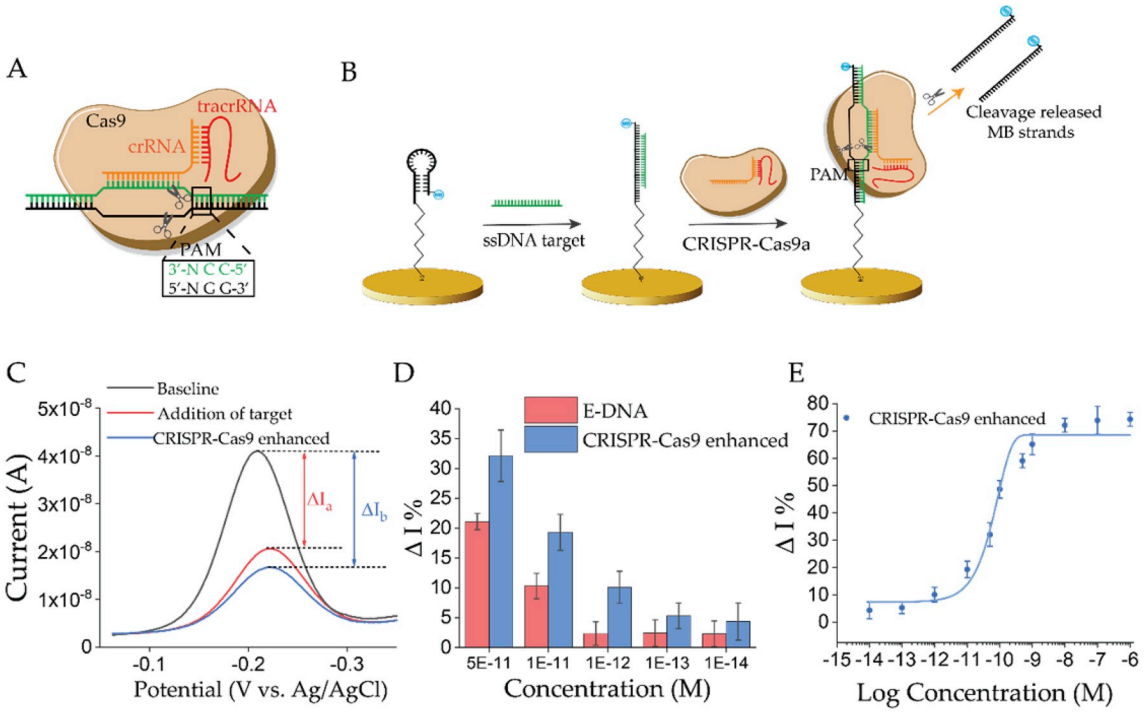

Fig. 2. Evaluation of the sensing performance of CRISPR-Cas9 enhanced E-DNA sensor. (A) CRISPR Cas9 system consists of Cas9 protein and tracerRNA and crRNA triplex. The combination of tracerRNA and crRNA is named guideRNA. Recognition of PAM sequence by Cas9 leads to crRNA guided dsDNA cleavage activity. (B) Workflow of CRISPR-Cas9 enhanced E-DNA sensor. (C) SWV (in response to 500 pM of target) comparison of baseline without the target (black), addition of ssDNA target (red) and CRISPR Cas9 enhanced result (blue). (D) ΔI%E-DNA= ($I_{baseline}$− $I_{addition\ of\ target}$)/$I_{baseline}$. ΔI%CRISPR enhanced = ($I_{baseline}$− $I_{CRISPR\ enhanced}$)/$I_{baseline}$. Comparison of detection limit between E-DNA sensor and CRISPR-Cas9 enhanced E-DNA sensor. (E) Dose-dependent response of CRISPR-Cas9 enhanced E-DNA sensor (SE = 3.2%). The data represents the mean ± S.E. of three replicates based on three individual sensors. (For interpretation of the references to colour in this figure legend, the reader is referred to the Web version of this article).

recognition motif for Cas12a depends on 5′ TTTN, which is different from that of the Cas9. Most importantly, upon the recognition of the complementary target through PAM confirmation and crRNA matching, Cas12a not only performs the cleavage activity on the target DNA (cis-cleavage), but also unleashes an indiscriminate single-stranded deoxyribonuclease activity (trans-cleavage) (Fig. 3A). This unique evolved property enhances the breakdown of the invading nucleic acids as an important part of the bacterial adaptive defense system of type V CRISPR enzyme (Gootenberg et al., 2018; Li et al., 2018). Therefore, we assumed that through the application of Cas12a′s cis and trans cleavage activities onto the E-DNA sensor, the detection limit and the dynamic detection range of E-DNA sensor can further be advanced.

Cas12a from *Lachnospiraceae* bacterium (LbCas12a) was selected for investigation owing to its superior enzymatic activity over that of the other Cas12a analogs (Dai et al., 2019b). Same experimental setting was applied for CRISPR-Cas12a enhanced E-DNA sensor as for CRISPR-Cas9 system (Fig. 3B). SWV demonstrated a more significant enhancement of signal gain by Cas12a system ($\Delta I_c\%$ = 67.5%) comparing with that of Cas9 ($\Delta I_b\%$ = 59.1%), indicating that the trans-cleavage activity of Cas12a might mediate the further decrease of the signal (Fig. 3C). To further understand the cleavage performance, we investigated the effect of divalent cation (Mg^{2+}) concentration in the *in vitro* cleavage solution because the RuvC catalytic domain is known to function the nuclease activity based on a two-metal ion mechanism (Yang, 2008). We only found that the presence of Mg^{2+} was critical to activation of the RuvC domain for the cleavage activity, but the variation of Mg^{2+} concentration did not demonstrate a noticeable effect on signal change for this sensing platform (Fig. S6). Another interesting finding is that the trans-cleavage activity is a continuous event after the activation of the cis-cleavage activity. The cis-cleavage activity is typically finished within 30 min (Chen et al., 2018; Gootenberg et al., 2018). However, our observation demonstrated that with the application of Cas12a, the current change kept increasing over 1 h (Fig. 3D). This phenomenon suggests that increasingthe CRISPR-Cas12a digestion period is a potential mean to tune the sensitivity and resolution for sensing applications. We further evaluated the dose-dependent response of the CRISPR-Cas12a enhanced E-DNA sensor for the detection range and the detection limit (Fig. 3E). An excellent dynamic range was found to cross 7 orders of magnitude. A saturated detection concentration was reached at 0.1 μM and an experimental detection limit was identified as 10 fM for both buffer and pooled human serum tests with an average standard error of 2.8%, indicating an excellent and stable detection performance. The linear detection range is identified as the whole pico-molar level (Fig. S7). Moreover, comparable IC50 values for buffer (31.9 pM) and pooled human serum test (51.6 pM) were acquired, indicating a potential operation of the developed CRISPR enhanced E-DNA sensor directly in complex biological fluids. The low matrix effect we observed may attribute to the CRISPR treatment process. For CRISPR enhancement procedure, it is necessary to use proteinase K, a serine protease (Zetsche et al., 2017), to treat the electrode in order to digest the Cas protein, retaining an electrode surface with nucleic acids only. Owing to the broad specificity of proteinase K as a proteinase, it would also digest those non-specifically, electrode absorbed proteins from human serum, therefore providing a comparable detection performance in complex matrix as in buffer. This observation also suggests that for surface chemistry mediated electrochemical biosensor development, a post-treatment through proteinase K may improve the detection performance on human biological samples.

3.4. Probing the mismatches with CRISPR enhanced DNA sensor

It would be of extremely high utility for a nucleic acid sensing system to be able to discriminate point mutation as a potential lab applicable technique for genotype screening. We firstly evaluated the mismatch

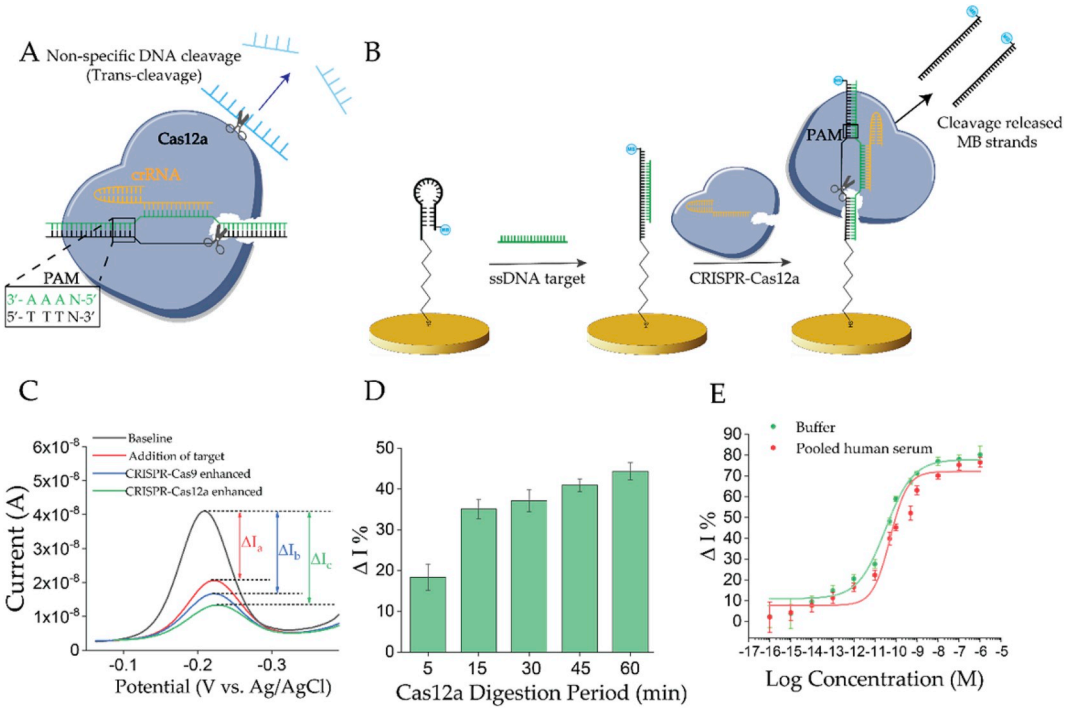

Fig. 3. Performance of CRISPR Cas12a enhanced E-DNA sensor. (A) CRISPR Cas12a-crRNA (yellow) duplex unit recognizes the PAM region, unwinds the dsDNA and binds the complementary strand (green). Recognition of dsDNA target activates its cis-cleavage activity, generating a 5′-overhang staggered cleavage. Activation of cis-cleavage activity further induces the trans-cleavage activity on non-specific DNA (blue). (B) Workflow of CRISPR-Cas12a enhanced E-DNA sensor. (C) SWV (in response to 500 pM target) comparison of baseline without the target (black), addition of ssDNA target (red), CRISPR Cas9 enhanced result (blue) and CRISPR Cas12a enhanced result (green). (D) $\Delta I\% = (I_{\text{addition of target}} - I_{\text{CRISPR-Cas12a enhanced}})/I_{\text{addition of target}}$. Enhancement of detection signal was observed with increasing period of the Cas12a digestion process. (E) Dose dependent responses based on the detection of ssDNA target in buffer and in pooled human serum ($\Delta I\%_{\text{CRISPR Cas12a enhanced}} = (I_{\text{baseline}} - I_{\text{CRISPR Cas12a enhanced}})/I_{\text{baseline}}$, SE = 2.73%) The data represent the mean ± S.E. of three replicates based on three individual sensors. (For interpretation of the references to colour in this figure legend, the reader is referred to the Web version of this article).

tolerance capability of E-DNA sensor based on the condition with only target induced conformational change. We artificially designed mutations at different locations of the target sequence (Table S1). 500 pM of each designed target was applied to the E-DNA sensor and the signal gains were compared without application of CRISPR systems (Fig. 4A). Same as wild type target, point mutations also led to the increase of current change of the E-DNA sensor because of the following reasons: 1. hairpin probe would still undergo conformational change because single mismatch is not able to significantly impede the nucleic acid hybridization process due to the similar melting temperatures of the hybridized dsDNAs (Table S1) (Kelley et al., 1999). 2. Other than the contact-mediated electron transfer process, the DNA mediated electron transfer process is also important for the intensity of the electrochemical signal (Pheeney and Barton, 2012). For analysis of targets with point mutation, after hybridization, due to the perturbation of the DNA base stacking by the mismatched base pair, DNA-mediated charge transduction is interfered (Slinker et al., 2011; Zwang et al., 2018), resulting in a decrease of electrochemical current and hence a higher % change

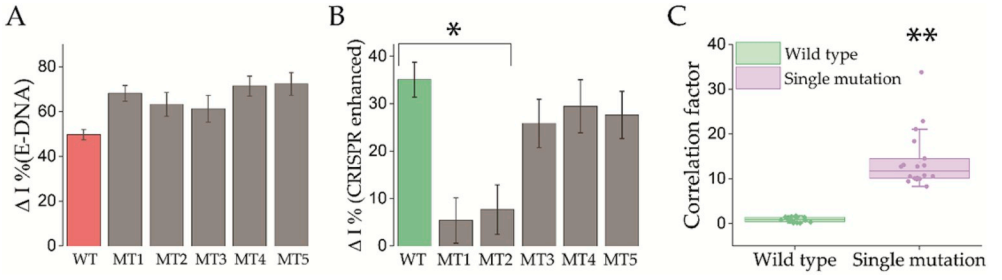

Fig. 4. Sequence dependent CRISPR cleavage activity for discrimination of point mutations. (A) Different target sequences with mutations at different positions induced current change based on the conformational change of hairpin probe of the E-DNA sensor. (B) Different target sequences with mutations at different positions induced current change based on the CRISPR cleavage activity after formation the target-hairpin dsDNA (n = 3, *P < 0.05, WT vs. MT1&MT2) (C) Correlation factor is based on E-DNA signal over CRISPR cleavage signal (Correlation factor=(ΔI%E-DNA)/ (ΔI %CRISPR enhanced)). The data for correlation factor was acquired based on triplet repeat of 5 different concentrations of wild type sequence or single mutation sequence testing on the E-DNA signal and CRISPR enhanced signal (n = 3, *P < 0.05, Single mutation vs. Wild type). The data represent the mean ± S.E. of three replicates based on three individual sensors.

before and after hybridization onto the E-DNA sensor. Actually, the variation of pi-stacking conformation in the dsDNA resulted unfavorable electron transfer through DNA has been utilized to identify point mutations in electrochemical biosensing systems (Boon et al., 2000; Furst et al., 2018; Zwang et al., 2018). However, these assays can only compare the electrochemistry of the mismatched strand with the well-matched strand based on a known target-concentration condition. Because, at the condition of unknown target-concentration, either high concentration of wild type target or mutated target can result a decrease of current output (Fig. S8). Thus, a general method, which is able to confirm that the decrease of current is created by the mutation without knowing the concentration, can be extremely meaningful for all types of nucleic acid sensing systems aiming to discriminate mutations.

Owing to the target complementarity dependent CRISPR cleavage activity, we hypothesized that the acquisition of CRISPR cleavage signal may provide a mean to identify the mutation in the sequence. After the targets hybridized on the E-DNA sensors, we examined the change of current ($\Delta I\%_{CRISPR\ enhanced} = (I_{addition\ of\ target} - I_{CRISPR\text{-}Cas12a\ enhanced})/I_{addition\ of\ target}$) caused by CRISPR cleavage activity based on different target sequences (Fig. 4B). Mutation 1 (MT1) and mutation 2 (MT2) are mismatched base pairs at PAM region and the PAM adjacent region corresponding to the crRNA of CRISPR Cas12a, which demonstrated significant attenuation of CRISPR cleavage activity. The demonstrated cleavage activity of mutated targets also matches previous presentation on the mismatched tolerance study of Cas12a (Kim et al., 2016). This phenomenon can be explained based on the CRISPR recognition dependent cleavage mechanism as described following: CRISPR Cas12a-crRNA duplex recognizes corresponding DNA target through a two-step process (Swarts et al., 2017). First, the Cas12a endonuclease searches for its corresponding PAM sequence (5′-TTTN). Upon the confirmation of the PAM sequence, the Cas12a endonuclease would unwind the double strand DNA. The second step involves the programmable crRNA to examine the complementarity between itself and the target. Once the target complementarity is confirmed, the RuvC domain of CRISPR will perform the cleavage activity. Therefore, mutations at PAM or PAM adjacent base pairs can avoid the CRISPR unwinding activity on the wrong targets, providing an effective mean to differentiate mutated sequences from the wild type sequence.

Based on this mutation dependent cleavage performance, we correlated the signal change of CRISPR cleavage activity with the signal change caused by E-DNA sensor. Utilizing this numerical correlation, we can indicate whether a mutated target sequence or a well-matched target sequence induces the electrical signal change, presenting a generalized method to examine the credibility of the detection result. The signal change based on E-DNA conformational change (ΔI%E-DNA) and the signal change by CRISPR cleavage (ΔI%CRISPR enhanced) of various concentrations (pM-nM) of the wild type target were firstly characterized. A correlation factor based on (ΔI%E-DNA)/ (ΔI%CRISPR enhanced) was then obtained with an average factor of 0.903 (green box chart, Fig. 4C). Same characterization process was also applied to different concentrations of mutation sequences (MT1 and MT2). The correlation factor was obtained with an average value of 11.731 (purple box chart). The significant difference of the correlated factors between the wild type target and targets with single mutations demonstrated the reliability of this method to examine the credibility of the detection result, enhancing the detection accuracy. This strategy simply involves CRISPR to perform a complementarity dependent cleavage activity as a second-time target recognition, which can be generalized to various hybridization based nucleic acid detection platform.

As demonstrated, CRISPR mediated stem-loop probe based nucleic acid biosensing construct is a generalizable, amplification-free, high-sensitivity and high-accuracy biosensing strategy. Still, some limitations need to be addressed for further researches. First, currently, the detection set-up is based on a signal-off assay, which might limit the dynamic detection range (Wang and Ma, 2019). Therefore, potential researches can be the design of CRISPR mediated signal-on biosensing strategy, which might lead to a lower detection limit. Second, CRISPR, as a ribonucleoprotein, has a limited binding affinity (~pM) toward nucleic acids target (O'Connell et al., 2014). Therefore, further developments on increasing the CRISPR binding affinity through engineered RNA can be extremely beneficial for biosensing researches.

4. Conclusion

In conclusion, we demonstrate a CRISPR enhanced nucleic acid detection strategy based on the E-DNA biosensing platform. Our approach exploits the specificity and the target complementarity dependent CRISPR enzymatic activity, surpassing the detection limit and most importantly, detection accuracy of the conventional electrochemical DNA sensors. Integration and correlation of the E-DNA sensor capturing signal and CRISPR cleavage signal lead to a dose-independent indication of the potential single-mutation in the target sequence, providing a reliable and universal method to examine the detection accuracy. Overall, these novel insights can be generalized to many nucleic acids biosensing platforms, promoting the development of biosensors one step forward toward robust point-of-care systems and clinically applicable genotype screenings.

Declaration of competing interest

The authors declare that they have no known competing financial interests or personal relationships that could have appeared to influence the work reported in this paper.

CRediT authorship contribution statement

Wei Xu: Formal analysis, Investigation, Validation. **Tian Jin:** Investigation, Validation. **Yifan Dai:** Conceptualization, Methodology, Writing - original draft, Writing - review & editing. **Chung Chiun Liu:** Supervision, Project administration.

Acknowledgements

We acknowledge the support from Wallace R Persons Research Fund from Case Western Reserve Univeristy. We thank the experimental assitances provided by the Electronics Design Center of Case Western Reserve University. We thank F. Zhang and X. Cao for their advice and support of this project.

Appendix A. Supplementary data

Supplementary data to this article can be found online at https://doi.org/10.1016/j.bios.2020.112100.

References

Arroyo-Currás, N., Dauphin-Ducharme, P., Ortega, G., Ploense, K.L., Kippin, T.E., Plaxco, K.W., 2018. ACS Sens. 3 (2), 360–366.
Blair, E.O., Corrigan, D.K., 2019. Biosens. Bioelectron. 134, 57–67.
Boon, E.M., Ceres, D.M., Drummond, T.G., Hill, M.G., Barton, J.K., 2000. Nat. Biotechnol. 18 (10), 1096–1100.
Bruch, R., Baaske, J., Chatelle, C., Meirich, M., Madlener, S., Weber, W., Dincer, C., Urban, G.A., 2019. Adv. Mater. 31 (51), 1905311.
Chen, J.S., Doudna, J.A., 2017. Nat. Rev. Chem. 1 (10), 78.
Chen, J.S., Ma, E., Harrington, L.B., Da Costa, M., Tian, X., Palefsky, J.M., Doudna, J.A., 2018. Science 360 (6387), 436–439.
Dai, Y., Furst, A., Liu, C.C., 2019a. Trends Biotechnol. 37 (12), 1367–1382.
Dai, Y., Liu, C.C., 2019. Angew. Chem. Int. Ed. 58 (36), 12355–12368.
Dai, Y., Somoza, R.A., Wang, L., Welter, J.F., Li, Y., Caplan, A.I., Liu, C.C., 2019b. Angew. Chem. Int. Ed. 58 (48), 17399–17405.
Dai, Y., Wang, C., Chiu, L.-Y., Abbasi, K., Tolbert, B.S., Sauvé, G., Yen, Y., Liu, C.-C., 2018. Biosens. Bioelectron. 117, 60–67.
Dauphin-Ducharme, P., Arroyo-Currás, N., Plaxco, K.W., 2019. J. Am. Chem. Soc. 141 (3), 1304–1311.
Dauphin-Ducharme, P., Plaxco, K.W., 2016. Anal. Chem. 88 (23), 11654–11662.
English, M.A., Soenksen, L.R., Gayet, R.V., de Puig, H., Angenent-Mari, N.M., Mao, A.S., Nguyen, P.Q., Collins, J.J., 2019. Science 365 (6455), 780–785.

Fan, C., Plaxco, K.W., Heeger, A.J., 2003. Proc. Natl. Acad. Sci. Unit. States Am. 100 (16), 9134–9137.
Fan, C., Plaxco, K.W., Heeger, A.J., 2005. Trends Biotechnol. 23 (4), 186–192.
Ferguson, B.S., Hoggarth, D.A., Maliniak, D., Ploense, K., White, R.J., Woodward, N., Hsieh, K., Bonham, A.J., Eisenstein, M., Kippin, T.E., Plaxco, K.W., Soh, H.T., 2013. Sci. Transl. Med. 5 (213), 213ra165.
Furst, A., Landefeld, S., Hill, M.G., Barton, J.K., 2013. J. Am. Chem. Soc. 135 (51), 19099–19102.
Furst, A.L., Muren, N.B., Hill, M.G., Barton, J.K., 2014. Proc. Natl. Acad. Sci. Unit. States Am. 111 (42), 14985–14989.
Furst, A.L., Smith, M.J., Lee, M.C., Francis, M.B., 2018. ACS Cent. Sci. 4 (7), 880–884.
Gootenberg, J.S., Abudayyeh, O.O., Kellner, M.J., Joung, J., Collins, J.J., Zhang, F., 2018. Science 360 (6387), 439–444.
Gootenberg, J.S., Abudayyeh, O.O., Lee, J.W., Essletzbichler, P., Dy, A.J., Joung, J., Verdine, V., Donghia, N., Daringer, N.M., Freije, C.A., 2017. Science 356 (6336), 438–442.
Hsieh, K., Patterson, A.S., Ferguson, B.S., Plaxco, K.W., Soh, H.T., 2012. Angew. Chem. Int. Ed. 51 (20), 4896–4900.
Hsu, P.D., Lander, E.S., Zhang, F., 2014. Cell 157 (6), 1262–1278.
Jinek, M., Chylinski, K., Fonfara, I., Hauer, M., Doudna, J.A., Charpentier, E., 2012. Science 337 (6096), 816–821.
Kang, D., Parolo, C., Sun, S., Ogden, N.E., Dahlquist, F.W., Plaxco, K.W., 2018. ACS Sens. 3 (7), 1271–1275.
Kang, D., Vallée-Bélisle, A., Porchetta, A., Plaxco, K.W., Ricci, F., 2012. Angew. Chem. Int. Ed. 51 (27), 6717–6721.
Kelley, S.O., Boon, E.M., Barton, J.K., Jackson, N.M., Hill, M.G., 1999. Nucleic Acids Res. 27 (24), 4830–4837.
Kelley, S.O., Mirkin, C.A., Walt, D.R., Ismagilov, R.F., Toner, M., Sargent, E.H., 2014. Nat. Nanotechnol. 9 (12), 969.
Kim, H.K., Song, M., Lee, J., Menon, A.V., Jung, S., Kang, Y.-M., Choi, J.W., Woo, E., Koh, H.C., Nam, J.-W., Kim, H., 2016. Nat. Methods 14, 153.
Kim, J., Campbell, A.S., de Ávila, B.E.-F., Wang, J., 2019. Nat. Biotechnol. 37 (4), 389–406.
Labib, M., Sargent, E.H., Kelley, S.O., 2016. Chem. Rev. 116 (16), 9001–9090.
Li, D., Song, S., Fan, C., 2010. Acc. Chem. Res. 43 (5), 631–641.
Li, H., Arroyo-Currás, N., Kang, D., Ricci, F., Plaxco, K.W., 2016. J. Am. Chem. Soc. 138 (49), 15809–15812.
Li, H., Dauphin-Ducharme, P., Ortega, G., Plaxco, K.W., 2017. J. Am. Chem. Soc. 139 (32), 11207–11213.
Li, M., Chen, T., Gooding, J.J., Liu, J., 2019. ACS Sens. 4 (7), 1732–1748.
Li, S.-Y., Cheng, Q.-X., Liu, J.-K., Nie, X.-Q., Zhao, G.-P., Wang, J., 2018. Cell Res. 28 (4), 491.
Lubin, A.A., Plaxco, K.W., 2010. Acc. Chem. Res. 43 (4), 496–505.
Mali, P., Yang, L., Esvelt, K.M., Aach, J., Guell, M., DiCarlo, J.E., Norville, J.E., Church, G.M., 2013. Science 339 (6121), 823–826.
Ng, P.C., Murray, S.S., Levy, S., Venter, J.C., 2009. Nature 461 (7265), 724.
O'Connell, M.R., Oakes, B.L., Sternberg, S.H., East-Seletsky, A., Kaplan, M., Doudna, J.A., 2014. Nature 516 (7530), 263–266.
Pan, Y., Hu, N., Wei, X., Gong, L., Zhang, B., Wan, H., Wang, P., 2019. Biosens. Bioelectron. 130, 344–351.
Pardee, K., Green, A.A., Takahashi, M.K., Braff, D., Lambert, G., Lee, J.W., Ferrante, T., Ma, D., Donghia, N., Fan, M., Daringer, N.M., Bosch, I., Dudley, D.M., O'Connor, D. H., Gehrke, L., Collins, J.J., 2016. Cell 165 (5), 1255–1266.
Pheeney, C.G., Barton, J.K., 2012. Langmuir 28 (17), 7063–7070.
Povedano, E., Valverde, A., Montiel, V.R.V., Pedrero, M., Yáñez-Sedeño, P., Barderas, R., San Segundo-Acosta, P., Peláez-García, A., Mendiola, M., Hardisson, D., 2018. Angew. Chem. 130 (27), 8326–8330.
Slinker, J.D., Muren, N.B., Renfrew, S.E., Barton, J.K., 2011. Nat. Chem. 3 (3), 228–233.
Song, S., Wang, L., Li, J., Fan, C., Zhao, J., 2008. Trac. Trends Anal. Chem. 27 (2), 108–117.
Sundaresan, R., Parameshwaran, H.P., Yogesha, S., Keilbarth, M.W., Rajan, R., 2017. Cell Rep. 21 (13), 3728–3739.
Swarts, D.C., van der Oost, J., Jinek, M., 2017. Mol. Cell 66 (2), 221–233 e224.
Vallée-Bélisle, A., Ricci, F., Uzawa, T., Xia, F., Plaxco, K.W., 2012. J. Am. Chem. Soc. 134 (37), 15197–15200.
Wang, H., Ma, Z., 2019. Biosens. Bioelectron. 132, 265–270.
Wei, X., Qin, C., Gu, C., He, C., Yuan, Q., Liu, M., Zhuang, L., Wan, H., Wang, P., 2019. Biosens. Bioelectron. 145, 111673.
White, R.J., Phares, N., Lubin, A.A., Xiao, Y., Plaxco, K.W., 2008. Langmuir 24 (18), 10513–10518.
White, R.J., Plaxco, K.W., 2010. Anal. Chem. 82 (1), 73–76.
Yang, W., 2008. Nat. Struct. Mol. Biol. 15, 1228.
Yang, Y., Gao, W., 2019. Chem. Soc. Rev. 48 (6), 1465–1491.
Young, N.S., Brown, K.E., 2004. N. Engl. J. Med. 350 (6), 586–597.
Zetsche, B., Gootenberg, Jonathan S., Abudayyeh, Omar O., Slaymaker, Ian M., Makarova, Kira S., Essletzbichler, P., Volz, Sara E., Joung, J., van der Oost, J., Regev, A., Koonin, Eugene V., Zhang, F., 2015. Cell 163 (3), 759–771.
Zetsche, B., Heidenreich, M., Mohanraju, P., Fedorova, I., Kneppers, J., DeGennaro, E.M., Winblad, N., Choudhury, S.R., Abudayyeh, O.O., Gootenberg, J.S., 2017. Nat. Biotechnol. 35 (1), 31.
Zuo, X., Song, S., Zhang, J., Pan, D., Wang, L., Fan, C., 2007. J. Am. Chem. Soc. 129 (5), 1042–1043.
Zwang, T.J., Tse, E.C.M., Barton, J.K., 2018. ACS Chem. Biol. 13 (7), 1799–1809.